



Citation for published version:

Borrelli, R & Dolgov, S 2021, 'Expanding the Range of Hierarchical Equations of Motion by Tensor-Train Implementation', *Journal of Physical Chemistry B*, vol. 125, no. 20, pp. 5397-5407.
<https://doi.org/10.1021/acs.jpcc.1c02724>

DOI:

[10.1021/acs.jpcc.1c02724](https://doi.org/10.1021/acs.jpcc.1c02724)

Publication date:

2021

Document Version

Peer reviewed version

[Link to publication](#)

This document is the Accepted Manuscript version of a Published Work that appeared in final form in *J. Phys. Chem. B*, copyright © American Chemical Society after peer review and technical editing by the publisher. To access the final edited and published work see <https://pubs.acs.org/doi/10.1021/acs.jpcc.1c02724>

University of Bath

Alternative formats

If you require this document in an alternative format, please contact:
openaccess@bath.ac.uk

General rights

Copyright and moral rights for the publications made accessible in the public portal are retained by the authors and/or other copyright owners and it is a condition of accessing publications that users recognise and abide by the legal requirements associated with these rights.

Take down policy

If you believe that this document breaches copyright please contact us providing details, and we will remove access to the work immediately and investigate your claim.

Expanding the Range of Hierarchical Equations of Motion by Tensor-Train Implementation

Raffaele Borrelli^{*,†} and Sergey Dolgov^{*,‡}

[†]*DISAFA, University of Torino, Largo Paolo Braccini 2, Grugliasco 10095 IT*

[‡]*University of Bath, Claverton Down, BA2 7AY Bath, United Kingdom*

E-mail: raffaele.borrelli@unito.it; s.dolgov@bath.ac.uk

Abstract

The Non-Equilibrium Thermo-Field Dynamics formulation of the Hierarchical Equations of Motion combined with the Tensor-Train representation of the density matrix is discussed, and a new numerical integration scheme is introduced. The numerical methodology is based on an adaptive low rank Galerkin reduction scheme and can preserve linear invariants (such as the trace of the density matrix). The method is applied to the study of the charge transfer dynamics in model pentacene molecular aggregates. The combined effect of a discrete set of molecular vibrational modes and of a thermal bath is investigated with special attention to the coherent-incoherent transition of the charge transport. The new computational framework is shown to be a very promising methodology for the study of quantum dynamics of complex molecular systems in condensed phase.

Introduction

The numerical simulation of time-dependent molecular processes is a cornerstone of modern theoretical chemistry, as it can unravel the complex mechanisms of elementary processes such as electron and energy transfer in molecular assemblies, which are of central importance for most present-day technologies for energy storage and transduction. Due to the inherent complexity of the systems of chemical interests, and to their interaction with a condensed phase, quite often the starting point of any time-dependent theoretical analysis is the identification of a relevant system part and an irrelevant environment. Their mutual coupling can then be treated at different level of approximations leading to several well known approaches based on the time-evolution of the reduced system density matrix.¹⁻⁵ It was only in the early '90 that Tanimura and Kubo⁶⁻⁸ developed the so-called Hierarchical Equation of Motion (HEOM) methodology, which remains one of the most important theoretical achievements in the study of the quantum dynamics of open systems enabling an exact description of the system-environment interaction. Since then, the HEOM technique has been applied to a variety of chemico-physical problems including charge-transfer,⁹ exciton dynamics,^{10,11} proton coupled electron-transfer,¹² and heat transport problems.¹³ (For a recent review of HEOM applications see ref.¹⁴).

Yet, the study of systems with a large number of degrees of freedom (DoF), such as molecular aggregates in a liquid or solid phase, using HEOM theory remains a challenging problem which has led to the implementation of several of numerical techniques capable of dealing with fairly complex systems.¹⁵⁻¹⁷ However, most of these methodologies have already hit their inherent limit and a leap towards a new paradigm is required in order to apply HEOM to study more realistic systems.

To tackle this problem, we have recently developed a new theoretical framework in which HEOM are derived using the so-called Non-Equilibrium Thermo-Field Dynamics (NETFD) (also referred to as twin-space formalism), and the resulting auxiliary density operator is approximated using the Tensor-Train (TT) decomposition.¹⁸ The use of TT approach to

solve HEOM has first been suggested by Shi and coworkers,¹⁹ and later by the Borrelli²⁰ and appears to be a very promising methodology to extend the range of applicability of HEOM.

In both cases the adopted integration scheme was based on the Dirac-Frenkel Time-Dependent Variational Principle (TDVP).²¹ This method determines the best approximation of a time-dependent vector in TT format by projecting the initial value problem onto a tangent space of a given manifold \mathcal{M} of TT tensors of fixed rank. Since the TT rank is preserved at all times the accuracy of the solution must be checked *a posteriori* by performing several calculations of increasing ranks. Moreover, the combination of this approach with HEOM violates norm and energy conservation of the solution,^{22,23} since the tangent space of \mathcal{M} does not contain the energy and trace operators automatically.

In this paper we address this problem by analysing the NETFD-TT approach to HEOM, and suggesting the application of a higher-order technique for the numerical time integration of the TT decomposition²⁴ which is adaptive in both TT ranks and time steps, and which is able to preserve the conservation laws of the system by incorporating them explicitly into the TT format.

Hierarchical Equation of Motion in NETFD formalism

In this section we provide the derivation of the HEOM using the NETFD formulation of quantum statistical mechanics.^{25–29} This approach to quantum statistical mechanics has long been known but only recently it has found the due attention in the theoretical chemistry community.^{30–36} Here, we will only briefly recall the formal structure of NETFD; more details are provided in the Appendix.

Let us consider a system described by a Hamiltonian operator H defined in the Hilbert space \mathcal{H} whose states are labelled as $\{|k\rangle\}$. Introduce a new operator \tilde{H} called *tildian* which has the same formal structure of the physical Hamiltonian but acts on a different Hilbert space $\tilde{\mathcal{H}}$ whose states are labelled as $\{|\tilde{k}\rangle\}$. Consider now the space obtained by the

Kronecker product $\mathcal{H} \otimes \tilde{\mathcal{H}}$ and its states $\{|i\tilde{j}\rangle = |i\rangle \otimes |\tilde{j}\rangle\}$ and define the vector $|\mathbf{1}\rangle$

$$|\mathbf{1}\rangle = \sum_k |k\tilde{k}\rangle \quad (1)$$

(boldface symbols emphasize that we deal with both physical and tilde states) and the state

$$|\rho(t)\rangle = \rho(t) |\mathbf{1}\rangle \quad (2)$$

where $\rho(t)$ is the density matrix of the original system. With this formal structure it is possible to demonstrate that the time evolution of the state $|\rho(t)\rangle$ is determined by the NETFD equation

$$\frac{\partial}{\partial t} |\rho(t)\rangle = -i(H - \tilde{H}) |\rho(t)\rangle = -i\hat{H} |\rho(t)\rangle \quad |\rho(0)\rangle = |\rho_0\rangle = \rho_0 |\mathbf{1}\rangle \quad (3)$$

($\hbar = 1$), and the expectation value of any operator U acting in the physical Hilbert space $\{|k\rangle\}$ can be obtained as

$$\langle U(t) \rangle = \langle \mathbf{1} | U | \psi(t) \rangle \equiv \text{Tr}\{\rho(t)U\}. \quad (4)$$

The evaluation of $\langle U(t) \rangle$ via the "wave function" $|\rho(t)\rangle$ or via the corresponding density matrix $\rho(t)$ are equivalent. The operator \hat{H} is also referred to as Liouvillian super-operator.

Using the NETFD formalism it is possible to define a reduced state vector analogous to the familiar reduced density matrix. This was first discussed by Arimitsu and Umezawa³⁷ using projection operator techniques and lead to a set of equations which share the same structure of the standard reduced density matrix approaches, but makes explicit use of tilde operators. Here we will briefly report its derivation, and then present a new formulation of an exact second-order cumulant approach based on a hierachical solver (see infra).⁶

Let us consider a system described by a Hamiltonian operator

$$H = \tilde{H}_A + \tilde{H}_B + V = H_0 + V \quad (5)$$

where A is the subsystem of interest, B the “bath” i.e. the irrelevant subsystem, V their coupling, and $H_0 = H_A + H_B$. The Liouville super-operator is thus given by

$$\hat{H} = H_A + H_B + V - \tilde{H}_A - \tilde{H}_B - \tilde{V} = \hat{H}_A + \hat{H}_B + \hat{V} = \hat{H}_0 + \hat{V} \quad (6)$$

where $\hat{H}_A = H_A - \tilde{H}_A$ and so on. The reduced state $|\rho_A(t)\rangle_I$ in the interaction representation can be defined by tracing out the bath degrees of freedom as

$$|\rho_A(t)\rangle_I = \langle 1_B | \rho(t) \rangle_I = e^{i\hat{H}_A t} \langle 1_B | \rho(t) \rangle = e^{i\hat{H}_A t} |\rho_A(t)\rangle. \quad (7)$$

where the unit vector $|1_B\rangle$ is defined as in eq. (1) but the summation includes only the states of the B subsystem.

We now make use of the key assumptions of HEOM theory, that is i) the system-bath interaction is factorized as

$$V = \sum_k S_k Q_k \quad (8)$$

where S_k and Q_k are system and bath operators respectively and ii) the bath operators are described as a linear combination of position operators q_j of harmonic oscillators

$$Q_k = \sum_j g_{kj} q_j. \quad (9)$$

Under this conditions it is possible to demonstrate that^{38,39}

$$|\rho_A(t)\rangle_I = T_+ \exp \left(- \int_0^t \hat{K}_I^{(2)}(s) ds \right) |\rho(0)\rangle_I. \quad (10)$$

where

$$\hat{K}_I^{(2)}(s) = \int_0^s d\tau \langle \hat{V}(s) \hat{V}(\tau) \rangle. \quad (11)$$

The average operation is defined as $\langle \dots \rangle = \langle 1_B | \dots | \rho_B(0) \rangle$ and $\hat{V}(t)$ is the interaction representation of the coupling super-operator $\hat{V} = \sum_k S_k Q_k - \sum_k \tilde{S}_k \tilde{Q}_k$.

Differentiating the above expression one obtains⁴⁰

$$\frac{\partial}{\partial t} |\rho_A(t)\rangle_I = -T_+ \int_0^t d\tau \langle \hat{V}(t) \hat{V}(\tau) \rangle \exp\left(-\int_0^t \hat{K}_I^{(2)}(s) ds\right) |\rho(0)\rangle_I. \quad (12)$$

It is fundamental to note that the variable τ in the integral above ranges over all times, so that, for $\tau < s$ the time ordering operator mixes $\hat{V}(\tau)$ with all the terms of the expansion of the exponential operator $\exp\left(-\int_0^t \hat{K}_I^{(2)}(s) ds\right)$, making it impossible to obtain an explicit equation for $|\rho_A(t)\rangle_I$. The hierarchical equation of motion represents a methodology to disentangle the above equation in the special case of a Gaussian bath. After some easy manipulations the second order cumulant can be written as²⁰

$$\hat{K}_I^{(2)}(t) = \sum_k [S_k(t) - \tilde{S}_k(t)] \left\{ \int_0^t dt_1 \langle Q_k(t) Q_k(t_1) \rangle S_k(t_1) - \int_0^t dt_1 \langle Q_k(t_1) Q_k(t) \rangle \tilde{S}_k(t_1) \right\}. \quad (13)$$

Taking advantage of the conjugation relation $\langle Q_k(t_1) Q_k(t) \rangle = \langle Q_k(t) Q_k(t_1) \rangle^*$ it is possible to write

$$\hat{K}_I^{(2)}(t) = \sum_k [S_k(t) - \tilde{S}_k(t)] \left\{ \int_0^t dt_1 C'_k(t-t_1) [S_k(t_1) - \tilde{S}_k(t_1)] - i \int_0^t dt_1 C''_k(t-t_1) [S_k(t_1) + \tilde{S}_k(t_1)] \right\} \quad (14)$$

where

$$C'_k(t-t_1) = \Re \langle Q_k(t_1) Q_k(t) \rangle \quad C''_k(t-t_1) = \Im \langle Q_k(t_1) Q_k(t) \rangle. \quad (15)$$

In the limit of a continuous distribution of frequencies we obtain the relations^{41,42}

$$C'_k(t-t_1) = \frac{1}{\pi} \int_0^\infty d\omega J_k(\omega) \coth(\beta\omega/2) \cos(\omega(t_1-t)) \quad C''_k(t-t_1) = \frac{1}{\pi} \int_0^\infty d\omega J_k(\omega) \sin(\omega(t_1-t)) \quad (16)$$

where $J_k(\omega)$ is the spectral density describing the system-bath interaction strength as a function of the bath frequency ω . These are well know results of time auto-correlation function theory.⁴¹ At this point we model the system-bath interaction as a non-Markovian Gaussian process described by a Drude-Lorentz spectral density

$$J_k(\omega) = 2\lambda_k \frac{\omega\gamma_k}{\omega^2 + \gamma_k^2}. \quad (17)$$

Here the parameter λ_k defines the strength of the system-bath interaction while γ_k is a characteristic bath frequency. Introducing the super-operators

$$\hat{S}_k(t) = [S_k(t) - \tilde{S}_k(t)] \quad (18)$$

$$\hat{R}_{kj}(t) = c_{kj}S_k(t) - c_{kj}^*\tilde{S}_k(t) \quad (19)$$

where the coefficient c_{kj} are defined in such a way that

$$C_k(t-t_1) = C'_k(t-t_1) + iC''_k(t-t_1) = \sum_j c_{kj} e^{-\gamma_{kj}|t-t_1|} \quad (20)$$

the second order cumulant can be written as

$$\hat{K}_I^{(2)}(t) = \sum_{kj} \hat{S}_k(t) \int_0^t d\tau e^{-\gamma_{kj}|t-\tau|} \hat{R}_{kj}(\tau). \quad (21)$$

Following a standard approach we can now define a set of auxiliary density vectors (ADV)⁶

$$|\rho_A^{\mathbf{m}}(t)\rangle = T_+ \prod_{kj} (m_{kj}! |c_{kj}|^{m_{kj}})^{-1/2} \left(i \int_0^t dt_1 e^{-\gamma_k |t-t_1|} \hat{R}_{kj}(\tau) \right)^{m_{kj}} \exp \left(- \int_0^t \hat{K}_I^{(2)}(s) ds \right) |\rho_A(0)\rangle_I \quad (22)$$

where $\mathbf{m} = \{m_{kj}\}$ is a set of non-negative integers. Here, the index k labels the number of spectral densities and the index j labels the number of expansion terms in the expansion of each spectral density. If the system is characterized by M spectral densities each having K expansion terms, then we have $M \cdot K$ auxiliary spectral density vectors, and the indices k, j can assume the values $k = 1, 2, \dots, M$, and $j = 1, 2, \dots, K$. It is readily verified that the vector $|\rho_A(t)\rangle_I$, describing the physical state of our system, corresponds to the auxiliary state vector having all indices $m_{kj} = 0$, *i.e.* $|\rho_A(t)\rangle_I = |\rho_A^{\mathbf{0}}(t)\rangle$. The above definition takes into account the scaling originally proposed by Shi and coworkers which improves the numerical stability of the final system of equations.⁴³ HEOM are readily derived upon repeated differentiation of the $|\rho^{\mathbf{m}}\rangle$ with respect to time. Moving to the Schrödinger representation the set of equations

$$\begin{aligned} \frac{\partial}{\partial t} |\rho_A^{\mathbf{m}}\rangle = & - (i \hat{H}_A + \sum_{kj} m_{kj} \gamma_{kj}) |\rho_A^{\mathbf{m}}\rangle - i \sum_{kj} \sqrt{m_{kj} / |c_{kj}|} (c_{kj} S_k - c_{kj}^* \tilde{S}_k) \left| \rho_A^{\mathbf{m}-1_{kj}} \right\rangle \\ & - i \sum_{kj} \sqrt{(m_{kj} + 1) |c_{kj}|} (S_k - \tilde{S}_k) \left| \rho_A^{\mathbf{m}+1_{kj}} \right\rangle \quad (23) \end{aligned}$$

is obtained, where $\mathbf{m} \pm 1_{kj} = (m_{10}, \dots, m_{kj} \pm 1, \dots)$, and the explicit time dependence of the auxiliary vectors has been dropped. The price to pay for disentangling the time ordering operation of eq. (12) is that HEOM constitutes an infinite set of first-order ordinary differential equations. This means that equation 12 has just been replaced by a different type of problem. Fortunately, using the hierarchy it is possible to devise very efficient truncation schemes which allow to obtain highly accurate results with a finite system. The reader is referred to the original papers for the derivation of an optimal truncation scheme.^{7,44} In the above derivation we have not considered low-temperature corrections which can be included straightforwardly from a direct application of the original approach suggested by Ishizaki

and Tanimura.⁴⁴

The above equations resemble very closely the results of HEOM theory in the density matrix formalism (see for example Ref.³⁹), but here the commutators and anti-commutators are replaced by differences and sums of tilde and non-tilde operators. As we shall see in the next section, this results in several benefits for the numerical implementation of the propagator.

To further simplify the structure of the HEOMs we follow Tanimura⁴⁵ and introduce a set of vectors $|\mathbf{m}\rangle = |m_{10}m_{11}\dots m_{1K}m_{20}\dots m_{MK}\rangle$, and their corresponding boson-like creation-annihilation operators b_{kj}^+, b_{kj}^-

$$b_{kj}^+ |\mathbf{m}\rangle = \sqrt{(m_{kj} + 1)} |\mathbf{m} + 1_{kj}\rangle \quad b_{kj}^- |\mathbf{m}\rangle = \sqrt{m_{kj}} |\mathbf{m} - 1_{kj}\rangle \quad b_{kj}^+ b_{kj}^- |\mathbf{m}\rangle = m_{kj} |\mathbf{m}\rangle \quad (24)$$

and the vector

$$|\rho(t)\rangle = \sum_{\mathbf{m}} |\rho_A^{\mathbf{m}}(t)\rangle |\mathbf{m}\rangle \quad (25)$$

and rewrite the hierarchical equations of motion in the compact form

$$\frac{\partial}{\partial t} |\rho\rangle = \left(-i\hat{H}_A - \sum_{kj} \gamma_{kj} b_{kj}^+ b_{kj}^- - i \sum_{kj} \sqrt{|c_{kj}|} (S_k - \tilde{S}_k) b_{kj}^- - i \sum_{kj} \frac{(c_{kj} S_k - c_{kj}^* \tilde{S}_k)}{\sqrt{|c_{kj}|}} b_{kj}^+ \right) |\rho\rangle, \quad (26)$$

with the initial condition given by $|\rho(0)\rangle = |\rho_A(0)\rangle |\mathbf{0}\rangle$.

Tensor-Train representation of the Density Vector

We now show how to exploit the structure of eq. 26 and of the vector of eq.25 to solve the quantum dynamical problem using the TT format.^{18,21,46-51}

Let us first recall the basic principles of the TT decomposition by considering a generic

expression of a state of a N dimensional quantum system at time t in the form

$$|\rho(t)\rangle = \sum_{i_1, i_2, \dots, i_N} C_t(i_1, \dots, i_N) |i_1\rangle \otimes |i_2\rangle \cdots |i_N\rangle. \quad (27)$$

where $|i_k\rangle$ labels the basis states of the k th dynamical variable, and the elements $C_t(i_1, \dots, i_N)$ are complex numbers labeled by N indices. If we truncate the summation of each index i_k to a maximum value p_k the elements $C_t(i_1, \dots, i_N)$ represent a tensor of order N . The evaluation of the summation (27) requires the computation (and storage) of p^N terms, where p is the average size of the one-dimensional basis set, which becomes prohibitive for large N . Using the TT format, the tensor C_t is approximated as

$$C_t(i_1, \dots, i_N) \approx C^{(1)}(i_1)C^{(2)}(i_2) \cdots C^{(N)}(i_N) \quad (28)$$

where $C^{(k)}(i_k)$ is a $r_{k-1} \times r_k$ complex matrix, $k = 1, \dots, N$ (for the moment, let us drop the time variable for simplicity). In the explicit index notation

$$C_t(i_1, \dots, i_N) \approx \sum_{\alpha_0, \dots, \alpha_N=1}^{r_0, \dots, r_N} C_{\alpha_0, \alpha_1}^{(1)}(i_1) C_{\alpha_1, \alpha_2}^{(2)}(i_2) \cdots C_{\alpha_{N-1}, \alpha_N}^{(N)}(i_N). \quad (29)$$

The trailing indices α_0 and α_N are introduced for uniformity of notation, but to render the right hand side scalar, we always set $r_0 = r_N = 1$. The factors $C^{(k)}$ are three dimensional arrays, called *cores* of the TT decomposition. The dimensions r_k are called TT ranks. The TT decomposition (28) is also known under the name of the Matrix Product States (MPS)^{52,53} In the MPS language the TT ranks are referred to as *bond dimensions*. Using the TT decomposition (28) it is possible, at least in principle, to overcome most of the difficulties caused by the dimension of the problem. Indeed, the wave function is entirely defined by N arrays of dimensions $r_{k-1} \times p_k \times r_k$ thus requiring a storage dimension of the order Npr^2 .

Turning now to the representation of the state vector of eq. (25) in the TT format we

let d be the number of degrees of freedom of the Hamiltonian operator H_A , and assume that the dissipating environment is described using M uncorrelated spectral densities $J_k(\omega)$ each expanded into K Matsubara terms. Hence, the vector $|\rho(t)\rangle$ of eq. (25) can be considered as a tensor with $N = 2d + KM$ indices. For sake of simplicity, in the following we consider the high temperature limit of the bath and employ the only one Matsubara term for each spectral density, *i.e.* $K = 1$, the generalization to $K > 1$ having only a slightly more involved notation. Therefore, in eq. (29) the first $2d$ indices label the physical and tilde DoFs and the last M indices label the bath operators. We specify that only the component with $\{m_k = 0, k = 1, \dots, M\}$ is required for the computation of physical observables.

Once the density matrix is known it is possible to compute any expectation value via eq. (4) where the operator U must have a TT form. As an example, the norm of the reduced system density, ρ_A , can be easily computed as $\text{tr}(\rho_A) = \langle \theta | \rho \rangle = 1$ where the vector $|\theta\rangle$ is defined as

$$|\theta\rangle = \left(\sum_{i_1} |i_1\rangle |\tilde{i}_1\rangle \otimes \sum_{i_2} |i_2\rangle |\tilde{i}_2\rangle \otimes \dots \otimes \sum_{i_d} |i_d\rangle |\tilde{i}_d\rangle \right) \otimes |\mathbf{0}\rangle \quad (30)$$

where $|\mathbf{0}\rangle = |0_1\rangle |0_2\rangle \dots |0_M\rangle$ label the first component of the ADVs.

Time Evolution of Tensor Trains

Several techniques exist to compute the time evolution of TT/MPS.^{21,54–57} Recently the time-dependent variational approach has been applied to solve HEOM in TT format. This method solves the dynamical equations projected onto the manifold of the TT decomposition using a splitting scheme over the TT cores. This enables an accurate evolution with fixed TT ranks, and hence prescribed computational costs. However, this method may not preserve certain invariants of the solution, such as the norm and energy, which are conserved by the equation (26).²⁰ This problem has also been recently addressed by Shi and coworkers who suggested to adopt a modified version of the HEOM equations combined with an additional constrain to enforce norm preservation.⁵⁸

Here we employ a new methodology for TT integration recently proposed by Dolgov²⁴ referred to as Time-dependent Alternating Minimal Energy solver (tAMEn). This integration technique automatically adjusts the TT ranks of the solution during the evolution to achieve a prescribed accuracy, and can fulfill the norm conservation law and any other type of *a priori* known linear invariants of the differential equation exactly, provided the state defining the invariant admits an exact TT decomposition. We briefly sketch the basic ideas behind the tAMEn algorithm and leave the reader to the original paper²⁴ for the mathematical and numerical details.

Firstly, we discretise the state $|\rho(t)\rangle$ in time by introducing a basis of Lagrange polynomials $\{P_\ell(t)\}_{\ell=1}^L$, centered at the Chebyshev points $\{t_\ell\}_{\ell=1}^L \subset [0, T]$. This gives us an approximation

$$|\rho(t)\rangle \approx \sum_{\ell=1}^L \sum_{i_1, \dots, i_N} C_{t_\ell}(i_1, \dots, i_N) |i_1\rangle \otimes \dots \otimes |i_N\rangle P_\ell(t), \quad t \in (0, T], \quad 0 < t_1 < \dots < t_L = T.$$

The nodal coefficients $C_{t_\ell}(i_1, \dots, i_N)$ altogether can be collected into a tensor of order $N + 1$, which is approximated by a TT decomposition similar to (28),

$$C_{t_\ell}(i_1, \dots, i_N) \approx C^{(1)}(i_1)C^{(2)}(i_2) \dots C^{(N)}(i_N) \cdot C^{(N+1)}(\ell). \quad (31)$$

Similarly, the nodal states $|\rho(t_\ell)\rangle$ can be collected into a “superstate” $|\boldsymbol{\rho}\rangle$.

In turn, the time derivative in (26) can be cast onto the polynomials $P_\ell(t)$, resulting in the *differentiation matrix* with elements $D_{\ell, \ell'} = \frac{dP_{\ell'}}{dt}(t_\ell)$, $\ell, \ell' = 1, \dots, L$, which can be computed explicitly. Turning D into a superoperator $\hat{D} = D \otimes I$ (where I is the identity operator matching the size of $|\rho\rangle$), the differential equation (26) is approximated by an algebraic

equation

$$\hat{A}|\boldsymbol{\rho}\rangle = |\mathbf{b}\rangle, \quad \text{where} \quad (32)$$

$$\hat{A} = \hat{D} + i\hat{H}_A + \sum_{kj} \gamma_{kj} b_{kj}^+ b_{kj}^- + i \sum_{kj} \sqrt{|c_{kj}|} (S_k - \tilde{S}_k) b_{kj}^- + i \sum_{kj} \frac{(c_{kj} S_k - c_{kj}^* \tilde{S}_k)}{\sqrt{|c_{kj}|}} b_{kj}^+,$$

$$|\mathbf{b}\rangle = (D1_L) \otimes |\rho(0)\rangle,$$

where 1_L is a vector of ones of size L . Having solved this equation, we can interpolate $|\boldsymbol{\rho}\rangle$ at any sought time $t \in [0, T]$. The convergence of this approximation is analysed in the pseudospectral approximation theory,⁵⁹ together with an adaptive selection of the step size T or degree L .

The algebraic equation (32) can be solved using the Alternating Minimal Energy (AMEn) method,⁵¹ which builds upon the Alternating Linear Scheme (ALS).⁶⁰ A TT decomposition (31) can be rewritten as a subspace reduction problem by stretching the k th TT core into a vector $|c^{(k)}\rangle \in \mathbb{R}^{r_{k-1} p_k r_k}$ with elements $|c^{(k)}\rangle(\alpha_{k-1} i_k \alpha_k) = C_{\alpha_{k-1}, \alpha_k}^{(k)}(i_k)$, and by introducing the *frame* operator $\hat{C}_{\neq k} \in \mathbb{R}^{(p_1 \cdots p_N L) \times (r_{k-1} p_k r_k)}$ such that $\hat{C}_{\neq k} |c^{(k)}\rangle$ contains all elements $C_{t_\ell}(i_1, \dots, i_N)$ (for uniformity of notation, we can let $p_{N+1} = L$). A tedious but straightforward calculation shows that $\hat{C}_{\neq k}$ is constructed from all but k th TT cores.⁶⁰ Crucially, if both \hat{A} and C are represented in the TT format, the computation and solution of the Galerkin reduced system

$$\langle \hat{C}_{\neq k} | \hat{A} | \hat{C}_{\neq k} \rangle \cdot |c^{(k)}\rangle = \langle \hat{C}_{\neq k} | \mathbf{b} \rangle \quad (33)$$

is cheap, requiring at most $\mathcal{O}(Np^2r^3)$ operations. The ALS algorithm seeks a TT approximation to the solution of (32) by iterating over $k = 1, \dots, N + 1$, solving (33) in each step, and updating the k th TT core $C^{(k)}$ with the elements of $|c^{(k)}\rangle$.

The AMEn method⁵¹ empowers ALS with adaptive TT ranks and faster convergence by

additionally expanding $C^{(k)}$ by a TT core of the TT approximation of the residual

$$(|\mathbf{b}\rangle - \hat{A}|\boldsymbol{\rho}\rangle)(i_1, \dots, i_N, \ell) \approx C^{(1)}(i_1) \cdots C^{(k-1)}(i_{k-1}) Z^{(k)}(i_k) Z^{(k+1)}(i_{k+1}) \cdots Z^{(N+1)}(\ell),$$

where $|z^{(k)}\rangle = \langle \hat{Z}_{\neq k} | |\mathbf{b}\rangle - \hat{A}|\boldsymbol{\rho}\rangle \rangle$ can be computed by the secondary ALS iteration similar to (33). Further on, if the exact dynamics preserves a linear invariant $\langle \theta | \rho \rangle$ where

$$|\theta\rangle = \sum_{i_1, \dots, i_N} C^{(1)}(i_1) \cdots C^{(k-1)}(i_{k-1}) \Theta^{(k)}(i_k) \cdots \Theta^{(N)}(i_N) \cdot |i_1\rangle \otimes \cdots \otimes |i_N\rangle \quad (34)$$

admits a TT decomposition, tAMEn²⁴ expands $C^{(k)}$ also with $\Theta^{(k)}$. Altogether, after (33) is solved, we replace a pair of TT cores with their padded versions,

$$C^{(k)}(i_k) := \begin{bmatrix} C^{(k)}(i_k) & \Theta^{(k)}(i_k) & Z^{(k)}(i_k) \end{bmatrix}, \quad C^{(k+1)}(i_{k+1}) := \begin{bmatrix} C^{(k+1)}(i_{k+1}) \\ 0 \\ 0 \end{bmatrix}. \quad (35)$$

The zeros in $C^{(k+1)}$ preserve the whole tensor C (and hence the state $|\rho\rangle$ remains correct), but the extra terms in $C^{(k)}$ enrich the frame operator $\hat{C}_{\neq k+1}$ for the next iteration in two ways: firstly, the invariant-generating state $|\theta\rangle$ belongs to the column subspace of $\hat{C}_{\neq k+1}$ exactly, and hence $\langle \theta | \rho \rangle$ is preserved. This also allows us to write the TT decomposition of $|\theta\rangle$ (34) with the first $k-1$ TT cores being $C^{(1)}, \dots, C^{(k-1)}$, since those contain now exact bases for $|\theta\rangle$. Secondly, the global residual information supplied by $Z^{(k)}$ accelerates the convergence towards the true solution of (32). Before the expansion (35), we can also truncate the TT rank r_k by computing a truncated Singular Value Decomposition (SVD) of $C^{(k)}$.¹⁸ The combination of this truncation and expansion (35) allows the tAMEn algorithm to adapt TT ranks according to the desired error threshold.

An unsophisticated error analysis of the tAMEn algorithm leads to the SVD truncation and time discretisation errors accumulated every time step, which for linear A-stable

equations makes the total error bound linear in time. However, the majority of numerical experiments demonstrate a much milder behaviour with the error fluctuating within a constant interval for long periods of time. Moreover, the conservation laws are preserved with the machine precision independently of the time interval and TT rank truncation.

Charge Transfer Dynamics in Molecular Aggregates

We now show how to apply the methodology developed in the preceding sections to the study of charge-transfer (CT) processes in realistic models of molecular aggregates. These latter are assemblies of identical molecular subunits interacting via their electronic degrees of freedom. The nature of the electronic states and of their coupling, as well as their interaction with specific inter-molecular vibrations and with the environment are key features that control their behaviour, and can produce a rich variety of properties which are appealing for several scientific and technological applications such as opto-electronics,⁶¹ solar energy storage, electron- and hole-transport in solar cells and many others.⁶²

In the most general case different electronic states interact with the environment in different ways and the degrees of freedom involved in the system-environment interaction are often uncorrelated, furthermore the nuclear DoFs of the molecular subunits are usually described as a discrete ensemble of harmonic oscillators, linearly interacting with the electronic subsystem. This model can be mapped into a relatively simple system Hamiltonian operator, H_A , of the form

$$H_A = \sum_{n,m}^{N_e} \epsilon_{nm} |n\rangle \langle m| + \sum_{k=1}^F \frac{\omega_k}{2} (p_k^2 + q_k^2) + \sum_{n,k}^{N_e, F} g_k^{(n)} q_k |n\rangle \langle n|. \quad (36)$$

Here the indices n, m run over all possible N_e electronic states of the aggregate, ϵ_{nm} is the matrix of the electronic energies and couplings, p_k, q_k are the momentum and position operator of the k th inter-molecular vibration having frequency ω_k , the parameters $g_k^{(n)}$ account for the vibronic interaction between the oscillators and the electronic states, and F is the

number of vibrational DoFs.

Here we focus on the study of charge transport in one-dimensional aggregates with nearest-neighbour coupling, which are the simplest and certainly the most studied type of molecular assemblies.⁶³ More specifically, we consider linear chains of a model pentacene (Pc) units. In a chain of N units the m th monomer of the aggregate can be found either in its ground electronic state $|0\rangle_m$ or in its cation state $|(+)\rangle_m$; the electronic basis $\{|m\rangle\}$ of eq. 5 is constructed as the direct product of the "singly excited" manifold as

$$|m\rangle = |0\rangle_1 \otimes \dots |(+)\rangle_m \dots |0\rangle_N \quad (37)$$

i.e. it represents an electronic state with the positive charge localized on the m th site of the chain. The vibrational frequencies and the linear vibronic couplings of our model are given in table 1. The magnitude of the parameters $g_k^{(n)}$ depends on the difference of the equilibrium position of the k th oscillator of the pentacene unit in its neutral ground state and its cation form. The overall reorganization energy for the pair Pc/Pc⁺ is $\lambda_{CT} = \sum_k S_k \omega_k = 577 \text{ cm}^{-1}$, where $S_k = (g_k/\omega_k)^2/2$ is the so-called Huang-Rhys factor⁶⁴ of the k th vibrational mode. This latter values provide a direct measure of the Franck-Condon activity of the mode in the charge-transfer process.^{65–67}

Furthermore, each monomer is coupled to a thermal reservoir at 300 K; the system-bath coupling is described by the Debye spectral density with a characteristic frequency $\gamma = 50 \text{ cm}^{-1}$ (which corresponds to a relaxation time of about 100 fs), and an overall reorganization energy of 100 cm^{-1} . This latter value is close to theoretical estimates obtained from molecular dynamics simulations of pentacene crystals.⁶⁸ We study the charge transport for two different values of the electronic coupling: $\epsilon_{12} = 600 \text{ cm}^{-1}$, and $\epsilon_{12} = 300 \text{ cm}^{-1}$, which correspond to typical values of the transfer integral found along different directions of pentacene crystals.⁶⁹ In all simulations we assume that the system is initially found in the ground vibrational state of its neutral form and that one end of the chain is instantaneously brought into its cationic

form, triggering the charge motion along the chain.

Table 1: Vibrational frequencies ω_n , linear couplings $g_k^{(n)}$ and Huang-Rhys factors, S_k , of the 7 mode model of the pentacene unit. We omit the electronic state label since the vibronic couplings are the same for all units. All the parameters are expressed in cm^{-1} and have been taken from the literature.⁷⁰

ω_k	g_k	S_k
265.6	107.0	0.0811
823.7	-126.0	0.0117
1054.6	-178.2	0.0143
1195.4	-246.2	0.0212
1234.5	-467.9	0.0718
1443.2	819.7	0.1613
1572.8	761.2	0.1171

We start by analysing the CT dynamics in a pentacene homodimer. To better understand the numerical effort of this calculation we point out that this model comprises one electronic DoF, and 14 vibrational DoFs. Since in the NETFD formalism the number of physical variables is doubled we have a total of 30 physical and tilde DoFs. Furthermore, since each electronic state interacts with a specific environment, we have two additional bath variable defined in eq. 24. This results in a TT representation of the density vector with 32 indices. Clearly such a calculation could not be afforded with the standard numerical machinery of HEOM.⁷¹ All our calculations were performed on a dual socket 28 core machine equipped with Intel(R) Xeon(R) Gold 6132 CPU. The tAMEn code⁷² is written in MATLAB, and the time required for the pentacene-dimer calculation is about 10 hours.

In figure 1a) the electronic population of the initial state of the system (corresponding to the charge completely localized on the first site) is reported as a function of time for the two values of the electronic coupling. Both curves show several beatings which are the result of a strong interplay between the pure electronic coupling and the vibronic contributions.

In figures 1b,c) the real and imaginary part of the off-diagonal terms of the electronic reduced electronic density matrix are reported. After a reasonable amount of time it is expected that the system reaches thermal equilibrium and the density vector becomes stationary (and real). As can be seen from figure 1b,c) this is indeed the case since the imaginary part of

the off-diagonal term falls off at long times, and the real part reaches the constant value -0.4 for $\epsilon_{12} = 600 \text{ cm}^{-1}$ and -0.27 for $\epsilon_{12} = 300 \text{ cm}^{-1}$. Interestingly, the real part of $\rho_{12}(t)$ shows an apparently simple structure with a predominant oscillation having a period of about 27 fs. This contribution can be very likely attributed to the strong vibronic activity of the high frequency vibration of pentacene at 1572 cm^{-1} . However, a closer examination reveals a much more complex pattern, originating from all the Franck-Condon active vibrations.

A most important feature of the tAMEn algorithm is the capability to preserve linear invariants of the system, as the trace of the reduced density matrix, *i.e.* the norm of the density vector, throughout the evolution without the need to introduce artificial constraints into the equations of motion which might alter the fidelity of the solution. In figure 2a) the norm conservation error is reported as a function of time. The results clearly evidence that the conservation law is fulfilled to a high degree of accuracy at all times. We remind that previous attempts to solve HEOM equations in TT formant using the TDVP integrator^{20,58} have evidenced a major problem caused by the lack of norm conservation of the solution, which is solved by the tAMEn algorithm.

A second key property of the tAMEn methodology is the adaptivity of the TT rank during the time evolution. Figure 2b) shows the maximum rank of the solution as a function of time. For $\epsilon_{12} = 600 \text{ cm}^{-1}$, the maximum rank increases (almost linearly) for the first 150 fs reaching the value of 265 at 196 fs, and then it starts to slowly decrease, and after 1 ps the maximum TT rank is stable around 100. This behaviour is expected and caused by the dephasing and the relaxation induced by the system-bath interaction. Indeed, the rank describes the degree of entanglement of the system DoFs which is partly destroyed by the dissipation.⁷³ A similar behaviour is observed for $\epsilon_{12} = 300 \text{ cm}^{-1}$: the rank reaches a plateau value of 103 after 150 fs, and remains stable for a fairly long stretch of time, then, around 300 fs it start to slowly decay reaching a value of 52 after 1 ps.

A most noteworthy feature is that the decrease in the electronic coupling strongly reduces the maximum rank of the TT representation during the evolution, which is clearly associated

to a lower degree of entanglement. We also point out that the TDVP algorithm for obvious reasons cannot provide any information of this type and cannot take advantage of the intrinsic dissipative dynamics of an open system.

In order to better understand the effect of the dissipation on the system dynamics, and on the system-bath entanglement, the purity, *i.e.* the quantity $\text{Tr}\rho^2(t)$, of the pentacene dimer model is reported in figure 3a) as a function of time for the two values of the electronic coupling ϵ_{12} . In both cases the purity decreases rapidly at early times, and a transient oscillatory behaviour accompanied by an overall increasing trend is evident. For $\epsilon_{12} = 300 \text{ cm}^{-1}$ the purity reaches a plateau value of 0.66 after 600 fs, while for $\epsilon_{12} = 600 \text{ cm}^{-1}$ the purity reaches the value of 0.83 after 1 ps with a clear positive slope. The observed recovery of the initial purity can be related to the ratio λ/ϵ_{12} which indicates how strongly the system states are perturbed by the bath: the smaller the perturbation the higher the purity rebound.⁷⁴

The possibility to investigate the dynamics of larger systems using our HEOM-TT approach is further demonstrated in figure 4 where the CT dynamics of a linear tetramer of pentacene units is shown. The overall system includes 28 vibrational degrees of freedom and 4 uncorrelated thermal baths. The bath parameters are the same used in the previous simulations. In this case the overall number of degrees of freedom is 62, and the CPU time required for the calculation is about 25 hours. Figure 4a) shows the populations of the four electronic states as a function of time. At long times a splitting in the populations of the central and terminal sites is evident and caused by the open boundary structure of the chain. High frequency oscillations due to the undamped nature of the discrete system of oscillators are also evident.

Figure 4b) shows the real part of the six off-diagonal terms of the reduced electronic density matrix of the pentacene tetramer. The short time dynamics reveals large high frequency oscillations driven by the strong vibronic activity of the high frequency modes of the system. Again, at longer times the reduced density matrix becomes almost stationary as

expected due to the equilibration with the heat reservoir. We notice that adjacent sites have the largest (negative) values of the off-diagonal couplings ($\rho_{12}, \rho_{23}, \rho_{34}$) which is expected due to the nearest-neighbour interaction model. For the same reason the term ρ_{14} remains always very small. The imaginary part of the off-diagonal terms of the density matrix falls to zero, as expected, but still exhibits some oscillatory behaviour which indicates that complete thermal equilibrium occurs at longer times.

Figure 5a,b) show the error in norm preservation, and the maximum value of the rank of the TT representation of the density vector as a function of time. As for the pentacene dimer dynamics the norm is preserved to high degree of accuracy; TT rank increases for the first 170 fs reaching the value of 296, and then it starts to slowly decrease; after 1 ps the maximum TT rank is stable around 100. We underline that these two important results enable the study of long time dynamics even for realistic complex chemical systems.

Finally, the purity, of the pentacene tetramer model is reported in figure 3b) as a function of time. Similarly to the dimer model the purity decreases rapidly at early times, and it reaches a plateau value of 0.48 after 600 fs. However, in this case the transient oscillatory behaviour is much less pronounced probably due to the larger number of vibrational DoFs involved in the dynamics which providing a stronger dephasing mechanism.

Conclusions

We have shown that the twin-space formulation of HEOM combined with the TT representation of the auxiliary density vector (HEOM-TT) can be a very versatile tool for the study of vibronic problems including system-bath interactions which are ubiquitous in physical chemistry. The new tAMEn algorithm used in this work has two key features which makes it particularly appealing for HEOM-TT: i) it can preserve the norm of the reduced density matrix to a prescribed accuracy ii) it adapts the ranks of the solution during the time evolution. The possibility to fulfill conservation laws is certainly fundamental for any

meaningful simulation of a physical system. Unfortunately, it is known that the application of the TDVP formalism to the Liouville-von Neumann equation results in a time evolution that does not respect neither norm nor energy conservation. Heller was the first to suggest the introduction of an additional constraint in order to preserve the norm in a pure TDVP theory,²³ and Shi and coworkers have recently shown that it is actually possible to implement this approach in HEOM methodology.⁵⁸ The approach adopted here has the advantage of introducing conservation laws without the need to modify the equations of motion of the density matrix. We further note that the tAMEn algorithm can easily handle time-dependent system Hamiltonian enabling the study of complex driven system.

The rank adaptivity has the clear advantage of providing a solution with a prescribed accuracy at all times. While pure TDVP approaches guarantee that the solution remains in the manifold of TT with fixed rank, apparently enabling long time dynamics avoiding rank inflation due to entanglement growth, they do not guarantee that the long time solution is accurate. The side effect of such a fixed cost approach is that several calculations with increasing TT ranks are necessary in order to check the accuracy of the final solution. We finally mention that mixed approaches based on a combination of TT-TDVP and Krylov subspace techniques, that introduce a rank adaptation step into the TDVP integration, have also been implemented.⁷⁵ Work is in progress to assess the possibility to apply this new integrators to HEOM and compare them to the tAMEn algorithm.

Acknowledgements

RB is deeply indebted to Professor Yoshitaka Tanimura for enlightening discussions about HEOM formalism, and to Professor Maxim Gelin for his constant support on the development of this work. This project has received funding from the European Union's Horizon 2020 Research and Innovation Program under Grant Agreement No. 826013. The author further acknowledges the CINECA Award Nos. VEMPS-HP10CU4N9A and MATSEC-

HP10CTVK2K under the ISCRA initiative, for the availability of high-performance computing resources and support, the University of Torino for the local research funding Grant No. BORR-RILO-19-01.

Appendix: basic NETFD theory.

In NETFD a double Hilbert space is defined, also referred to as Liouville space, $\mathcal{L} = (\mathcal{H} \otimes \tilde{\mathcal{H}})$ where $\tilde{\mathcal{H}}$ is the Hilbert space of a fictitious dynamical system identical to the original Hilbert space \mathcal{H} of the real physical systems.^{28,29,76} If $\{|m\tilde{n}\rangle\}$ is an orthonormal basis of \mathcal{L} then

$$\langle m\tilde{n}|m'\tilde{n}'\rangle = \delta_{mm'}\delta_{\tilde{n}\tilde{n}'} \quad \sum_{m\tilde{n}} |m\tilde{n}\rangle \langle m\tilde{n}| = 1.$$

The identity vector $|I\rangle$ is further defined as

$$|I\rangle = \sum_m |m\tilde{m}\rangle. \quad (38)$$

This special vector allows to define a mapping between the dual space of \mathcal{H} (*i.e.* the bra space) and the tilde space, indeed we have

$$\langle m|I\rangle = |\tilde{m}\rangle \quad \langle \tilde{m}|I\rangle = |m\rangle. \quad (39)$$

Using this relations it is possible to associate a vector of the \mathcal{L} space to each operator A acting in the \mathcal{H} space

$$|A\rangle = A|I\rangle. \quad (40)$$

Similarly, we can define a state vector $|\rho(t)\rangle = \rho(t)|I\rangle$, where $\rho(t)$ is the density matrix of the system. Accordingly, the expectation value of A is defined as the scalar product

$$\langle A\rangle = \langle A|\rho(t)\rangle = \langle I|A\rho(t)|I\rangle \equiv \text{tr}(A\rho(t)). \quad (41)$$

The meaning of the above notation can be easily understood using the closure relation

$$|A\rangle = A|I\rangle = \sum_{mn} |m\tilde{n}\rangle \langle m\tilde{n}|A|I\rangle = \sum_{mn} \langle m|A|n\rangle |m\tilde{n}\rangle = \sum_{mn} A_{mn} |m\tilde{n}\rangle$$

whence it is clear that the vector $|A\rangle$ is a linear combination of a basis of \mathcal{L} with coefficients given by the matrix elements A_{mn} . Together with operators acting in the space \mathcal{H} it is possible to define a set of operators acting on the $\tilde{\mathcal{H}}$ space. In particular, following Suzuki,²⁸ two operators A and B are weakly equivalent if

$$A|I\rangle = B|I\rangle \quad (42)$$

and we write

$$A \simeq B. \quad (43)$$

For each Hermitian operator A acting in the \mathcal{H} space it is possible to define a tilde operator \tilde{A} that is weakly equivalent to A as

$$A|I\rangle = \tilde{A}^\dagger|I\rangle \longrightarrow A \simeq \tilde{A}^\dagger \quad (44)$$

where the dag operator implies the Hermitian conjugation. Consequently, for Hermitian operators

$$A \simeq \tilde{A}. \quad (45)$$

The tilde operator can be obtained from the original operators by the so-called tilde conjugation rules

$$(AB)^\sim = \tilde{A}\tilde{B} \quad (c_1A + c_2B)^\sim = c_1^*\tilde{A} + c_2^*\tilde{B}. \quad (46)$$

If A, B are two operators of the \mathcal{H} space and $\hat{A} = A - \tilde{A}^\dagger$ then

$$\hat{A}B|I\rangle = (A - \tilde{A}^\dagger)B|I\rangle = (AB - B\tilde{A}^\dagger)|I\rangle = (AB - BA)|I\rangle = [A, B]|I\rangle \quad (47)$$

proving the fundamental property of the twin-space formalism

$$[A, B] \simeq \hat{A}B. \quad (48)$$

References

- (1) Redfield, A. G. In *Advances in Magnetic and Optical Resonance*; Waugh, J. S., Ed.; Advances in Magnetic Resonance; Academic Press, 1965; Vol. 1; pp 1–32.
- (2) Lindblad, G. On the Generators of Quantum Dynamical Semigroups. *Commun. Math. Phys.* **1976**, *48*, 119–130.
- (3) Gelin, M. F.; Egorova, D.; Domcke, W. Exact Quantum Master Equation for a Molecular Aggregate Coupled to a Harmonic Bath. *Phys. Rev. E* **2011**, *84*, 041139.
- (4) Caldeira, A. O.; Leggett, A. J. Quantum Tunnelling in a Dissipative System. *Ann. Phys.* **1983**, *149*, 374–456.
- (5) Leggett, A. J.; Chakravarty, S.; Dorsey, A. T.; Fisher, M. P.; Zwerger, W. Dynamics of the Dissipative Two-State System. *Rev Mod Phys* **1987**, *59*, 1–85.
- (6) Tanimura, Y.; Kubo, R. Time Evolution of a Quantum System in Contact with a Nearly Gaussian-Markoffian Noise Bath. *J. Phys. Soc. Jpn.* **1989**, *58*, 101–114.
- (7) Tanimura, Y.; Kubo, R. Two-Time Correlation Functions of a System Coupled to a Heat Bath with a Gaussian-Markoffian Interaction. *J. Phys. Soc. Jpn.* **1989**, *58*, 1199–1206.
- (8) Tanimura, Y. Nonperturbative Expansion Method for a Quantum System Coupled to a Harmonic-Oscillator Bath. *Phys. Rev. A* **1990**, *41*, 6676–6687.
- (9) Tanimura, Y. Reduced Hierarchy Equations of Motion Approach with Drude plus Brownian Spectral Distribution: Probing Electron Transfer Processes by Means of Two-Dimensional Correlation Spectroscopy. *J. Chem. Phys.* **2012**, *137*, 22A550.

- (10) Sakamoto, S.; Tanimura, Y. Exciton-Coupled Electron Transfer Process Controlled by Non-Markovian Environments. *J. Phys. Chem. Lett.* **2017**, *8*, 5390–5394.
- (11) Ishizaki, A.; Fleming, G. R. Theoretical Examination of Quantum Coherence in a Photosynthetic System at Physiological Temperature. *PNAS* **2009**, *106*, 17255–17260.
- (12) Zhang, J.; Borrelli, R.; Tanimura, Y. Proton Tunneling in a Two-Dimensional Potential Energy Surface with a Non-Linear System–Bath Interaction: Thermal Suppression of Reaction Rate. *J. Chem. Phys.* **2020**, *152*, 214114.
- (13) Kato, A.; Tanimura, Y. Quantum Heat Current under Non-Perturbative and Non-Markovian Conditions: Applications to Heat Machines. *The Journal of Chemical Physics* **2016**, *145*, 224105.
- (14) Tanimura, Y. Numerically “Exact” Approach to Open Quantum Dynamics: The Hierarchical Equations of Motion (HEOM). *J. Chem. Phys.* **2020**, *153*, 020901.
- (15) Kreisbeck, C.; Kramer, T.; Rodríguez, M.; Hein, B. High-Performance Solution of Hierarchical Equations of Motion for Studying Energy Transfer in Light-Harvesting Complexes. *J. Chem. Theory Comput.* **2011**, *7*, 2166–2174.
- (16) Strümpfer, J.; Schulten, K. Light Harvesting Complex II B850 Excitation Dynamics. *J. Chem. Phys.* **2009**, *131*, 225101.
- (17) Strümpfer, J.; Schulten, K. Open Quantum Dynamics Calculations with the Hierarchy Equations of Motion on Parallel Computers. *J. Chem. Theory Comput.* **2012**, *8*, 2808–2816.
- (18) Oseledets, I. Tensor-Train Decomposition. *SIAM J. Sci. Comput.* **2011**, *33*, 2295–2317.
- (19) Shi, Q.; Xu, Y.; Yan, Y.; Xu, M. Efficient Propagation of the Hierarchical Equations of Motion Using the Matrix Product State Method. *The Journal of Chemical Physics* **2018**, *148*, 174102.

- (20) Borrelli, R. Density Matrix Dynamics in Twin-Formulation: An Efficient Methodology Based on Tensor-Train Representation of Reduced Equations of Motion. *J. Chem. Phys.* **2019**, *150*, 234102.
- (21) Lubich, C.; Oseledets, I.; Vandereycken, B. Time Integration of Tensor Trains. *SIAM J. Numer. Anal.* **2015**, *53*, 917–941.
- (22) McLachlan, A. A Variational Solution of the Time-Dependent Schrodinger Equation. *Mol. Phys.* **1964**, *8*, 39–44.
- (23) Heller, E. J. Time Dependent Variational Approach to Semiclassical Dynamics. *J. Chem. Phys.* **1976**, *64*, 63–73.
- (24) Dolgov, S. V. A Tensor Decomposition Algorithm for Large ODEs with Conservation Laws. *Comput. Methods Appl. Math.* **2019**, *19*, 23–38.
- (25) Umezawa, H.; Matsumoto, H.; Tachiki, M. *Thermo Field Dynamics and Condensed States*; North-Holland: Netherlands, 1982.
- (26) Takahashi, Y.; Umezawa, H. Thermo Field Dynamics. *Int. J. Mod. Phys. B* **1996**, *10*, 1755–1805.
- (27) Arimitsu, T.; Umezawa, H.; Yamanaka, Y. Canonical Formalism of Dissipative Fields in Thermo Field Dynamics. *J. Math. Phys.* **1987**, *28*, 2741–2752.
- (28) Suzuki, M. Density Matrix Formalism, Double-Space and Thermo Field Dynamics in Non-Equilibrium Dissipative Systems. *Int. J. Mod. Phys. B* **1991**, *05*, 1821–1842.
- (29) Schmutz, M. Real-Time Green’s Functions in Many Body Problems. *Z Physik B* **1978**, *30*, 97–106.
- (30) Borrelli, R.; Gelin, M. F. Quantum Electron-Vibrational Dynamics at Finite Temperature: Thermo Field Dynamics Approach. *J. Chem. Phys.* **2016**, *145*, 224101.

- (31) Gelin Maxim F.; Borrelli Raffaele, Thermal Schrödinger Equation: Efficient Tool for Simulation of Many-Body Quantum Dynamics at Finite Temperature. *Annalen der Physik* **2017**, *529*, 1700200.
- (32) Borrelli, R. Theoretical Study of Charge-Transfer Processes at Finite Temperature Using a Novel Thermal Schrödinger Equation. *Chemical Physics* **2018**, *515*, 236–241.
- (33) Borrelli, R.; Gelin, M. F. Simulation of Quantum Dynamics of Excitonic Systems at Finite Temperature: An Efficient Method Based on Thermo Field Dynamics. *Sci. Rep.* **2017**, *7*, 9127.
- (34) Begušić, T.; Vaníček, J. On-the-Fly Ab Initio Semiclassical Evaluation of Vibronic Spectra at Finite Temperature. *J. Chem. Phys.* **2020**, *153*, 024105.
- (35) Harsha, G.; Henderson, T. M.; Scuseria, G. E. Thermofield Theory for Finite-Temperature Quantum Chemistry. *J. Chem. Phys.* **2019**, *150*, 154109.
- (36) Harsha, G.; Henderson, T. M.; Scuseria, G. E. Thermofield Theory for Finite-Temperature Coupled Cluster. *J. Chem. Theory Comput.* **2019**, *15*, 6127–6136.
- (37) Arimitsu, T.; Umezawa, H. Non-Equilibrium Thermo Field Dynamics. *Prog. Theor. Phys.* **1987**, *77*, 32–52.
- (38) Kubo, R. Generalized Cumulant Expansion Method. *J. Phys. Soc. Jpn.* **1962**, *17*, 1100.
- (39) Ishizaki, A.; Calhoun, T. R.; Schlau-Cohen, G. S.; Fleming, G. R. Quantum Coherence and Its Interplay with Protein Environments in Photosynthetic Electronic Energy Transfer. *Phys. Chem. Chem. Phys.* **2010**, *12*, 7319–7337.
- (40) Jones, F. C.; Birmingham, T. J. When Is Quasi-Linear Theory Exact? *Plasma Phys.* **1975**, *17*, 15.
- (41) Mukamel, S. *Principles of Nonlinear Optical Spectroscopy*; Oxford University Press: Oxford, 1999.

- (42) Breuer, H.-P.; Petruccione, F. *The Theory of Open Quantum Systems*; Oxford University Press: Oxford [England]; New York, 2010.
- (43) Shi, Q.; Chen, L.; Nan, G.; Xu, R.-X.; Yan, Y. Efficient Hierarchical Liouville Space Propagator to Quantum Dissipative Dynamics. *J. Chem. Phys.* **2009**, *130*, 084105.
- (44) Ishizaki, A.; Tanimura, Y. Quantum Dynamics of System Strongly Coupled to Low-Temperature Colored Noise Bath: Reduced Hierarchy Equations Approach. *J. Phys. Soc. Jpn.* **2005**, *74*, 3131–3134.
- (45) Tanimura, Y. Stochastic Liouville, Langevin, Fokker–Planck, and Master Equation Approaches to Quantum Dissipative Systems. *J. Phys. Soc. Jpn.* **2006**, *75*, 082001.
- (46) Lubich, C.; Oseledets, I. V. A Projector-Splitting Integrator for Dynamical Low-Rank Approximation. *Bit Numer Math* **2013**, *54*, 171–188.
- (47) Oseledets, I.; Tyrtyshnikov, E. Breaking the Curse of Dimensionality, Or How to Use SVD in Many Dimensions. *SIAM J. Sci. Comput.* **2009**, *31*, 3744–3759.
- (48) Holtz, S.; Rohwedder, T.; Schneider, R. On Manifolds of Tensors of Fixed TT-Rank. *Numer. Math.* **2011**, *120*, 701–731.
- (49) Thomas, P. S.; Carrington, T. Using Nested Contractions and a Hierarchical Tensor Format To Compute Vibrational Spectra of Molecules with Seven Atoms. *J. Phys. Chem. A* **2015**, *119*, 13074–13091.
- (50) Dolgov, S.; Khoromskij, B.; Oseledets, I. Fast Solution of Parabolic Problems in the Tensor Train/Quantized Tensor Train Format with Initial Application to the Fokker–Planck Equation. *SIAM J. Sci. Comput.* **2012**, *34*, A3016–A3038.
- (51) Dolgov, S.; Savostyanov, D. Alternating Minimal Energy Methods for Linear Systems in Higher Dimensions. *SIAM J. Sci. Comput.* **2014**, *36*, A2248–A2271.

- (52) Fannes, M.; Nachtergaele, B.; Werner, R. F. Finitely Correlated States on Quantum Spin Chains. *Commun.Math. Phys.* **1992**, *144*, 443–490.
- (53) Perez-Garcia, D.; Verstraete, F.; Wolf, M. M.; Cirac, J. I. Matrix Product State Representations. *Quantum Info. Comput.* **2007**, *7*, 401–430.
- (54) Wall, M. L.; Carr, L. D. Out-of-Equilibrium Dynamics with Matrix Product States. *New J. Phys.* **2012**, *14*, 125015.
- (55) García-Ripoll, J. J. Time Evolution of Matrix Product States. *New J. Phys.* **2006**, *8*, 305.
- (56) Haegeman, J.; Lubich, C.; Oseledets, I.; Vandereycken, B.; Verstraete, F. Unifying Time Evolution and Optimization with Matrix Product States. *Phys. Rev. B* **2016**, *94*, 165116.
- (57) Paeckel, S.; Köhler, T.; Swoboda, A.; Manmana, S. R.; Schollwöck, U.; Hubig, C. Time-Evolution Methods for Matrix-Product States. *Annals of Physics* **2019**, *411*, 167998.
- (58) Yan, Y.; Xing, T.; Shi, Q. A New Method to Improve the Numerical Stability of the Hierarchical Equations of Motion for Discrete Harmonic Oscillator Modes. *J. Chem. Phys.* **2020**, *153*, 204109.
- (59) Trefethen, L. N. *Spectral Methods in MATLAB*; Society for Industrial and Applied Mathematics, 2000.
- (60) Holtz, S.; Rohwedder, T.; Schneider, R. The Alternating Linear Scheme for Tensor Optimization in the Tensor Train Format. *SIAM J. Sci. Comput.* **2012**, *34*, A683–A713.
- (61) Mei, J.; Diao, Y.; Appleton, A. L.; Fang, L.; Bao, Z. Integrated Materials Design of Organic Semiconductors for Field-Effect Transistors. *J. Am. Chem. Soc.* **2013**, *135*, 6724–6746.

- (62) Lu, L.; Zheng, T.; Wu, Q.; Schneider, A. M.; Zhao, D.; Yu, L. Recent Advances in Bulk Heterojunction Polymer Solar Cells. *Chem. Rev.* **2015**, *115*, 12666–12731.
- (63) Spano, F. C. Excitons in Conjugated Oligomer Aggregates, Films, and Crystals. *Annu. Rev. Phys. Chem.* **2006**, *57*, 217–243.
- (64) Huang, K.; Rhys, A. Theory of Light Absorption and Non-Radiative Transitions in F-Centres. *Proc. R. Soc. Lond. Ser. Math. Phys. Sci.* **1950**, *204*, 406–423.
- (65) Borrelli, R.; Di Donato, M.; Peluso, A. Quantum Dynamics of Electron Transfer from Bacteriochlorophyll to Pheophytin in Bacterial Reaction Centers. *J. Chem. Theory Comput.* **2007**, *3*, 673–680.
- (66) Borrelli, R.; Peluso, A. Perturbative Calculation of Franck–Condon Integrals: New Hints for a Rational Implementation. *J. Chem. Phys.* **2008**, *129*, 064116–7.
- (67) Borrelli, R.; Di Donato, M.; Peluso, A. Electron Transfer Rates and Franck–Condon Factors: An Application to the Early Electron Transfer Steps in Photosynthetic Reaction Centers. *Theor. Chem. Acc. Theory Comput. Model. Theor. Chim. Acta* **2007**, *117*, 957–967.
- (68) McMahon, D. P.; Troisi, A. Evaluation of the External Reorganization Energy of Polyacenes. *J. Phys. Chem. Lett.* **2010**, *1*, 941–946.
- (69) Landi, A.; Borrelli, R.; Capobianco, A.; Velardo, A.; Peluso, A. Second-Order Cumulant Approach for the Evaluation of Anisotropic Hole Mobility in Organic Semiconductors. *J. Phys. Chem. C* **2018**, *122*, 25849–25857.
- (70) Landi, A.; Borrelli, R.; Capobianco, A.; Velardo, A.; Peluso, A. Hole Hopping Rates in Organic Semiconductors: A Second-Order Cumulant Approach. *J. Chem. Theory Comput.* **2018**, *14*, 1594–1601.

- (71) Cainelli, M.; Tanimura, Y. Exciton Transfer in Organic Photovoltaic Cells: A Role of Local and Nonlocal Electron–Phonon Interactions in a Donor Domain. *J. Chem. Phys.* **2021**, *154*, 034107.
- (72) <https://github.com/dolgov/tamen>.
- (73) Somoza, A. D.; Marty, O.; Lim, J.; Huelga, S. F.; Plenio, M. B. Dissipation-Assisted Matrix Product Factorization. *Phys. Rev. Lett.* **2019**, *123*, 100502.
- (74) Chatterley, A. S.; Young, J. D.; Townsend, D.; Żurek, J. M.; Paterson, M. J.; Roberts, G. M.; Stavros, V. G. Manipulating Dynamics with Chemical Structure: Probing Vibrationally-Enhanced Tunnelling in Photoexcited Catechol. *Phys. Chem. Chem. Phys.* **2013**, *15*, 6879–6892.
- (75) Yang, M.; White, S. R. Time-Dependent Variational Principle with Ancillary Krylov Subspace. *Phys. Rev. B* **2020**, *102*, 094315.
- (76) Suzuki, M. Thermo Field Dynamics in Equilibrium and Non-Equilibrium Interacting Quantum Systems. *J. Phys. Soc. Jpn.* **1985**, *54*, 4483–4485.

Graphical TOC Entry

Insert graphical abstract




Figure 1: a) Charge-transfer dynamics in a pentacene homodimer; the charge is initially localized on site 1; $P_1(t)$ is the electronic occupation number of site 1; with. Bath reorganization energy is 100 cm^{-1} , characteristic frequency $\omega_c = 50 \text{ cm}^{-1}$. The hierarchy level is truncated at $m = 10$ on each bath. b) Real part of the off-diagonal term of the electronic reduced density matrix. c) Imaginary part of the off-diagonal term of the electronic reduced density matrix. Blue line $\epsilon_{12} = 600 \text{ cm}^{-1}$; red line $\epsilon_{12} = 300 \text{ cm}^{-1}$.

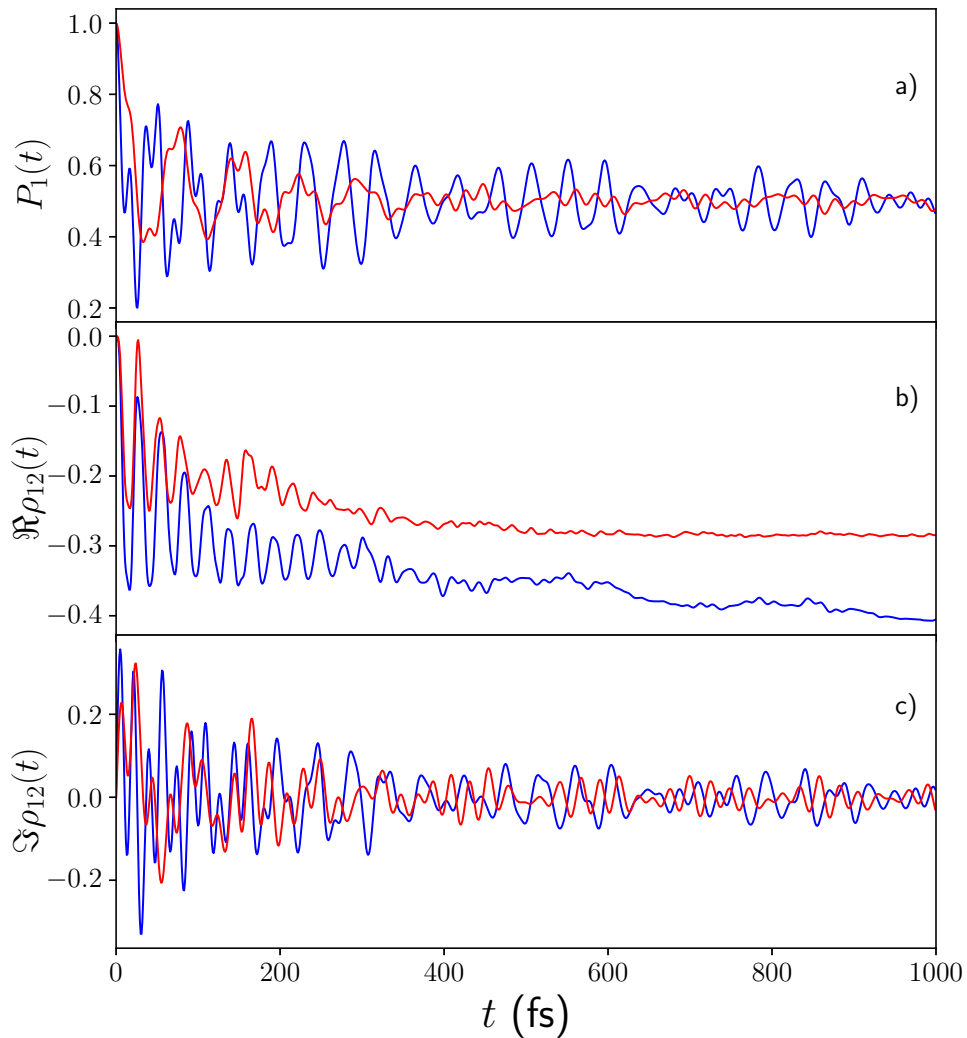


Figure 2: a) Error in the norm preservation of the density matrix during the evolution of the pentacene homodimer system. The parameters of the system are the same used for figure 1. b) Maximum value of the rank of the TT representation of the density matrix as a function of time. Blue line $\epsilon_{12} = 600 \text{ cm}^{-1}$; red line $\epsilon_{12} = 300 \text{ cm}^{-1}$.

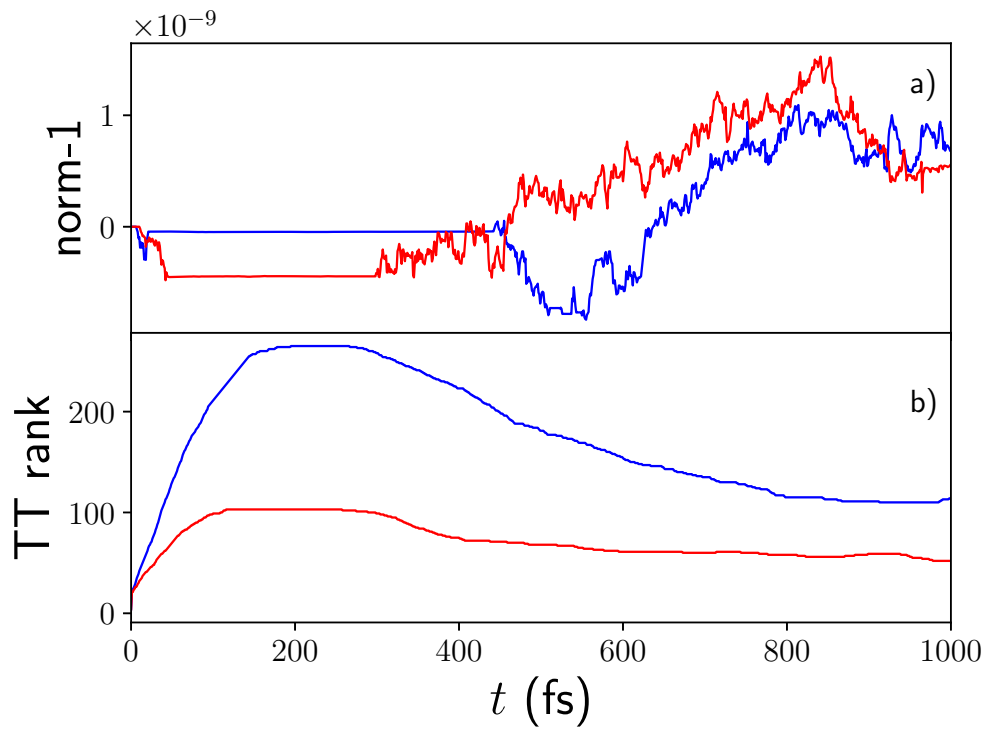


Figure 3: a) Purity of the vibronic model of the pentacene dimer coupled to a bath. Blue line $\epsilon_{12} = 600 \text{ cm}^{-1}$; red line $\epsilon_{12} = 300 \text{ cm}^{-1}$; b) Purity of the vibronic model of the pentacene tetramer coupled to a bath; bath reorganization energy 100 cm^{-1} , characteristic frequency $\omega_c = 50 \text{ cm}^{-1}$.

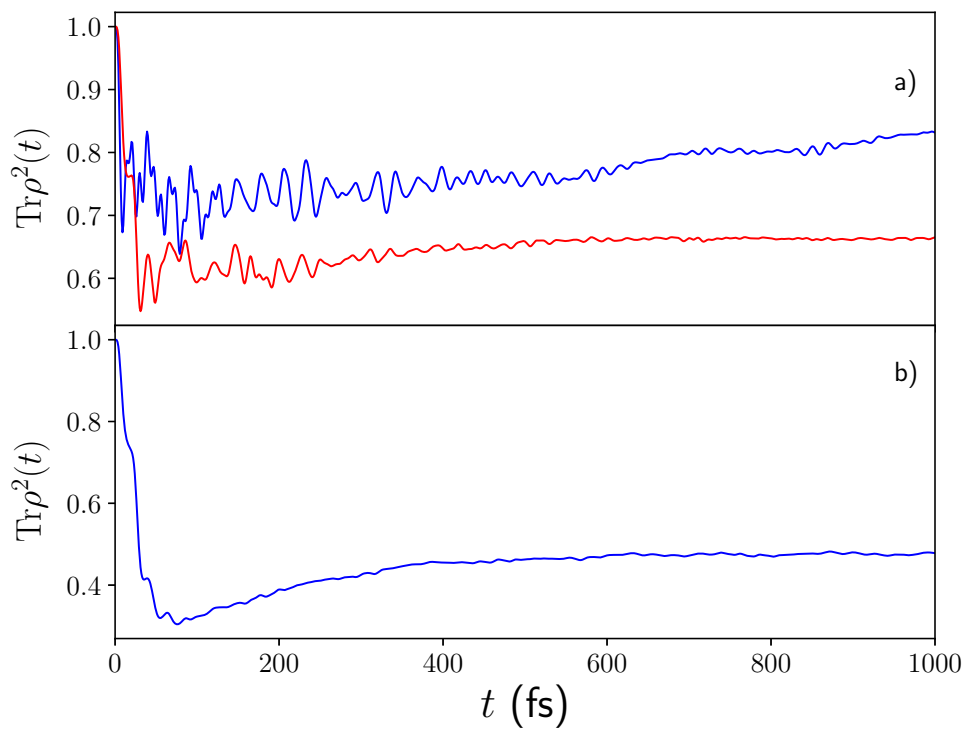


Figure 4: a) Charge-transfer dynamics in a pentacene tetramer; the charge is initially localized on site 1; p_k label the electronic occupation number of site k ; b) Real part of the off-diagonal term of the electronic reduced density matrix; c) Imaginary part of the off-diagonal term of the electronic reduced density matrix; Bath reorganization energy $\lambda = 100 \text{ cm}^{-1}$, bath characteristic frequency $\omega_c = 50 \text{ cm}^{-1}$, electronic coupling $\epsilon_{12} = 300 \text{ cm}^{-1}$. The hierarchy level is truncated at $m = 10$ on each bath.

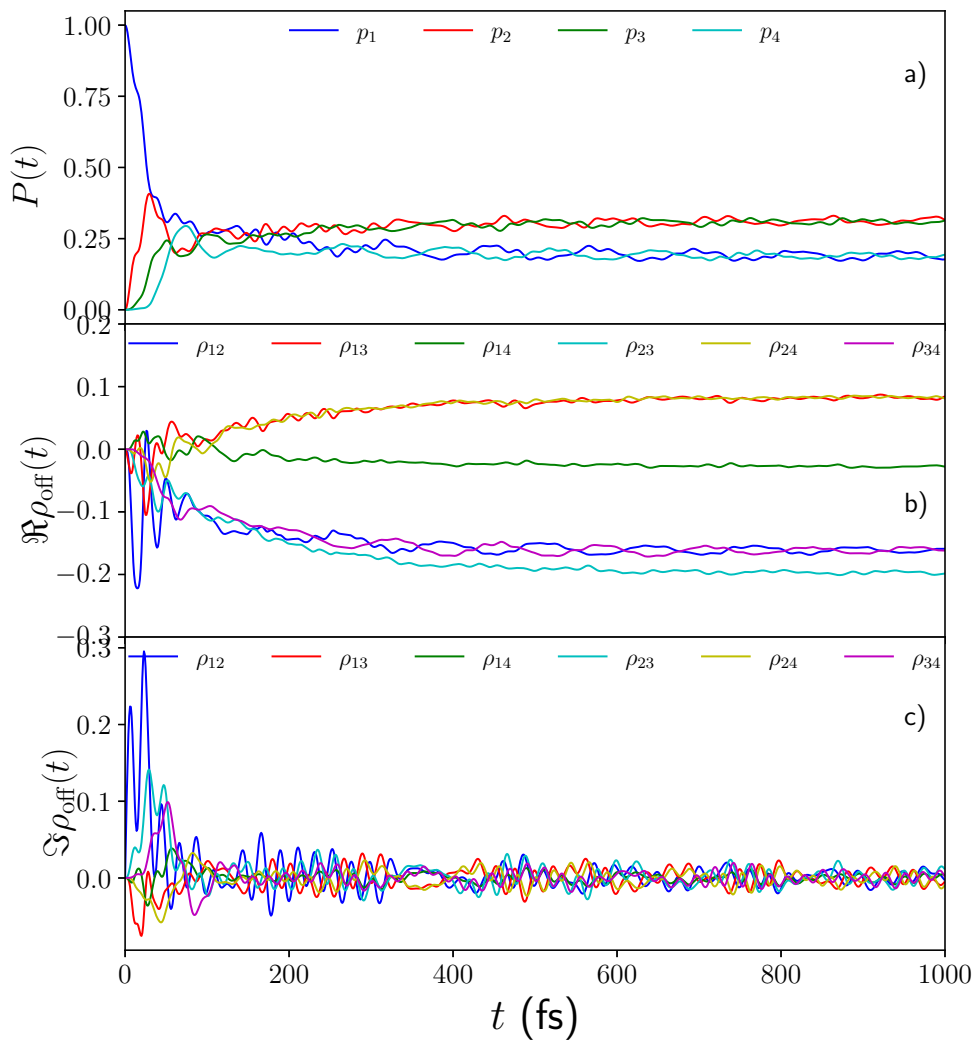


Figure 5: a) Error in the norm preservation of the density matrix during the evolution of the pentacene tetramer system. b) Maximum value of the rank of the TT representation of the density matrix as a function of time. Bath reorganization energy $\lambda = 100 \text{ cm}^{-1}$, bath characteristic frequency $\omega_c = 50 \text{ cm}^{-1}$, electronic coupling $\epsilon_{12} = 300 \text{ cm}^{-1}$. The hierarchy level is truncated at $m = 10$ on each bath.

